Bioorganic & Medicinal Chemistry Letters 23 (2013) 3438–3442

Contents lists available at SciVerse ScienceDirect

Bioorganic & Medicinal Chemistry Letters

journal homepage: www.elsevier.com/locate/bmcl

Discovery of potent, selective, bioavailable phosphodiesterase 2 (PDE2) inhibitors active in an osteoarthritis pain model, Part I: Transformation of selective pyrazolodiazepinone phosphodiesterase 4 (PDE4) inhibitors into selective PDE2 inhibitors

Mark S. Plummer [a,*], Joseph Cornicelli [b], Howard Roark [a], Donald J. Skalitzky [a], Charles J. Stankovic [d], Susan Bove [b], Jayvardhan Pandit [c], Annise Goodman [a], James Hicks [a], Aurash Shahripour [a], David Beidler [b], Xiao Kang Lu [b], Brian Sanchez [b], Christopher Whitehead [a], Ron Sarver [e], Timothy Braden [b], Richard Gowan [b], Xi Qiang Shen [b], Katherine Welch [b], Adam Ogden [d], Nalini Sadagopan [d], Heidi Baum [d], Howard Miller [d], Craig Banotai [e], Cindy Spessard [e], Sandra Lightle [e]

[a] Department of Chemistry, Pfizer Global Research and Development, Ann Arbor, MI 48105, USA
[b] Inflammation Pharmacology, Pfizer Global Research and Development, Ann Arbor, MI 48105, USA
[c] Discovery Technology, Pfizer Global Research and Development, Groton CT 06340, USA
[d] Pharmacodynamics and Drug Metabolism, Pfizer Global Research and Development, Ann Arbor, MI 48105, USA
[e] Discovery Technology, Pfizer Global Research and Development, Ann Arbor, MI 48105, USA

ARTICLE INFO

Article history:
Available online 28 March 2013

Keywords:
Phosphodiesterase 2 (PDE2)inhibition
Structure-based drug design
Osteoarthritis(OA)pain

ABSTRACT

We identified potent, selective PDE2 inhibitors by optimizing residual PDE2 activity in a series of PDE4 inhibitors, while simultaneously minimizing PDE4 activity. These newly designed PDE2 inhibitors bind to the PDE2 enzyme in a cGMP-like mode in contrast to the cAMP-like binding mode found in PDE4. Structure activity relationship studies coupled with an inhibitor bound crystal structure in the active site of the catalytic domain of PDE2 identified structural features required to minimize PDE4 inhibition while simultaneously maximizing PDE2 inhibition.

Despite the number of analgesic medicines and their various mechanisms of action, inflammatory pain is a condition that has significant unmet medical need and afflicts a large percentage of the population. This percentage will increase as the population ages. The efficacy of current medications is often limited and side effects can hinder utility.[1] Thus, it is important to identify new medicines with novel mechanisms of action to effectively treat patients with chronic pain. As part of an indications discovery effort to identify novel analgesic mechanisms, we observed antinociceptive activity in a selective phosphodiesterase 2 (PDE2) oxindole inhibitor **1**[2] (Scheme 1) in an acute model of inflammatory pain.

The role of PDE2 in the production and modulation of pain is inferred from a number of observations: (1) PDE2 is highly expressed in the brain, spinal cord, dorsal root ganglia (DRG), as well as non-pain related tissues including adrenal cortex, heart, and platelets,[3] (2) selective inhibition of PDE2 elevates cGMP in cells or subcellular compartments where it is located,[4] (3) the non-hydrolyzable cGMP analog, 8-bromo-cGMP, reduces nociceptive behavior in rats at low doses in formalin-induced inflammatory pain, but causes hyperalgesia when injected at higher doses.[5] In contrast to results obtained with oxindole **1**, EHNA (erythro-9-(2-hydroxy-3-nonyl)adenine) **2** (Figure 1), which is a weak inhibitor of PDE2, was reported to have no effect on nociceptive behavior,[5] (4) PDE2 mRNA expression, however, is increased after formalin injection.[6] To establish in vivo proof of concept in our animal models of OA pain we sought a nanomolar potent orally bioavailable PDE2 selective (>100× versus other PDEs) inhibitor that was non brain penetrant. Low brain penetration would avoid potential CNS side effects while allowing a PDE2 inhibitor to act at the DRG. Notably several organizations have actively pursued selective PDE2 inhibitors and their patent activity is reported in the Ref. and notes.

PDE2 is unique among the known 11 PDE isozymes as it has specificity for both cAMP and cGMP while being cGMP stimulated[8], such that increased concentrations of cGMP produce an increased rate of cAMP hydrolysis. The increase in enzyme activity is attributed to allosteric interactions initiated by the binding of cGMP to the GAF B domain of the enzyme.[7] Employing the apo crystal structure of the PDE2 catalytic domain enabled a structure based

* Corresponding author.
E-mail address: marksplummer@gmail.com (M.S. Plummer).

0960-894X/$ - see front matter © 2013 Elsevier Ltd. All rights reserved.
http://dx.doi.org/10.1016/j.bmcl.2013.03.072

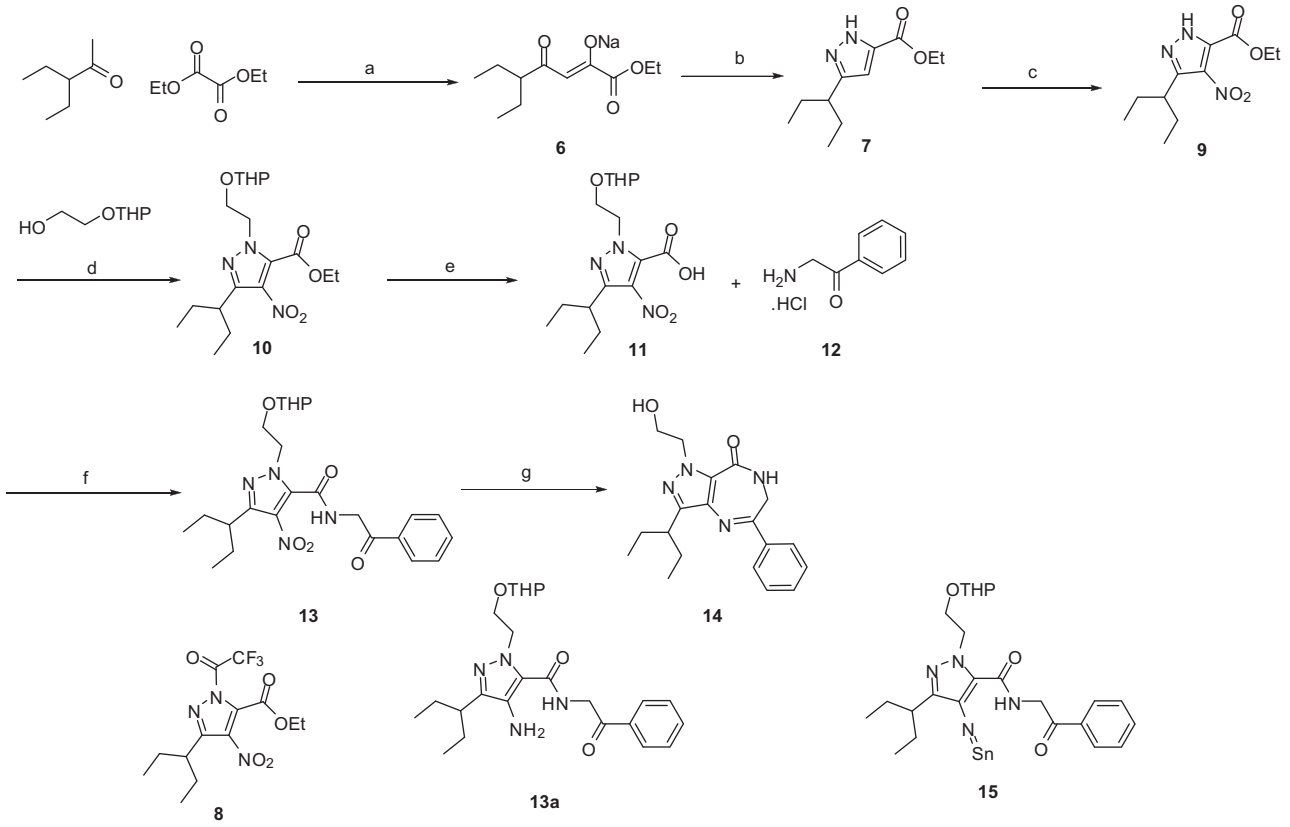

Scheme 1. (a) NaOEt/EtOH, (72%); (b) N_2H_4 H_2O, EtOH (98%); (c) $Cu(NO_3)_2$, $CHCl_3$/TFAA (90%): (d) resin-PPh_3/DIAD/0-RT (83%); (e) NaOH/MeOH/H_2O (100%); (f) EDAC HCl/HOBt/NMM/CH_2Cl_2 (76%); (g) $SnCl_2 2 \times H_2O$, EtOH/reflux (50%).

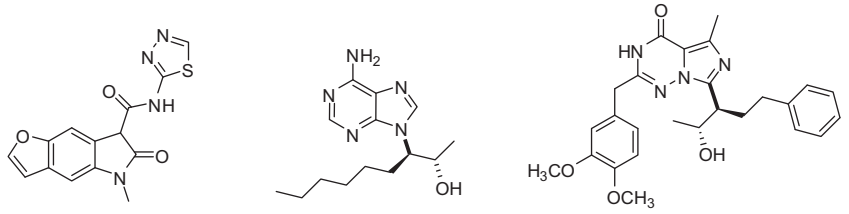

Figure 1. Known PDE2 inhibitors: oxindole[2], EHNA[7], and bay 60–7550.[8]

discovery program. We sought to establish selective PDE2 inhibition as a mechanism by which to treat inflammatory pain. Although the PDE2 selective oxindole **1** has many characteristics of an acceptable pharmacological inhibitor, we required alternative chemical matter with broader SAR and improved potency. A class of potent imidazotriazinone PDE2 inhibitors represented by Bay 60-7550 **3** show moderate to highly selective (50 to 800-fold) PDE2 inhibition and were also considered as lead chemical matter.[9] In vivo studies with this agent suggest it may have beneficial effects in cognitive disorders, however, **3** was discounted as a lead due to reported CNS effects and poor metabolic stability. Mining Pfizer's chemical database revealed a series of phosphodiesterase 4 (PDE4) diazepinone inhibitors[10] which often had low levels of PDE2 inhibition (Figure 2). Two diazepinones from the historic PDE4 program had advanced to become clinical candidates, and demonstrated excellent pharmacokinetic properties as represented by **4**.

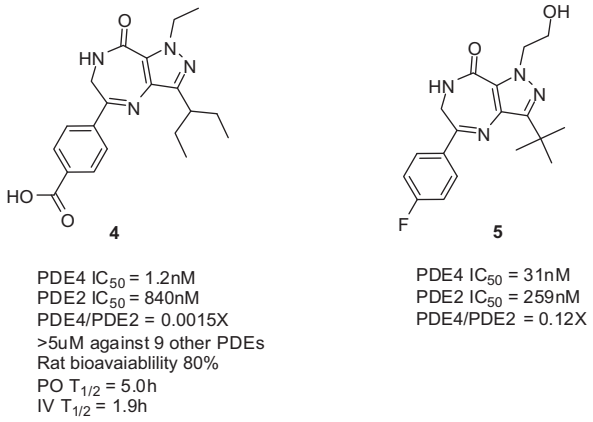

Figure 2. PDE4 inhibitors possessing residual PDE2 activity as starting points for the discovery of potent, selective PDE2 inhibitors.

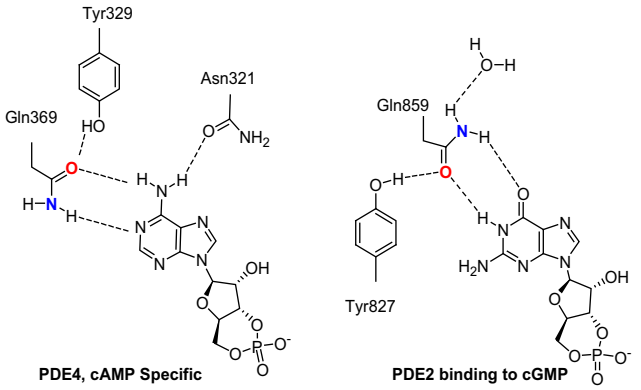

Figure 3. Modeled hydrogen bonding interactions of cAMP with PDE4, and cGMP with PDE2 showing the switch in orientation of the conserved glutamine.

Structure activity relationships (SAR) in the PDE4 diazepinone series indicated that good initial potency for PDE2 existed as shown by **5** (Figure 2). Additionally, PDE4 diazepinone inhibitors had been crystallized in the PDE4 catalytic domain and provided a strong basis for a future structure-enabled project once PDE2 cocrystals were obtained. Early demonstration of good PDE2 selectivity especially over the PDE4 isoforms was of importance to avoid severe emesis seen with PDE4 inhibition.

Since PDE4 specifically hydrolyzes cAMP, while PDE2 hydrolyzes both cAMP and cGMP, we postulated that the diazepinone-based inhibitors might bind in a unique mode to PDE2 relative to their binding mode to all of the PDE4 subtypes. After extensive modeling of diazepinone-based inhibitors in the active site of the PDE2 apo catalytic domain, we predicted that diazepinone inhibitors would bind to PDE2 in a cGMP-like binding mode, orthogonal to that found in the PDE4 subtypes due to alternative orientations of a key glutamine residue (Gln 859 in PDE2), referred to as the 'glutamine switch' (Figure 3).[11] This offered a strong basis for decreasing the undesired PDE4 activity while increasing PDE2 inhibition.

Compounds in this series were synthesized as shown in Scheme 1. 3-Ethyl heptanone was condensed with diethyl oxalate in ethanol to give the sodium salt **6** which was neutralized with aqueous hydrochloric acid and treated with hydrazine hydrate at 0 °C to provide pyrazole **7**. Pyrazole **7** was nitrated in chloroform with copper(II) nitrate and trifluoroacetic anhydride. This procedure provided the intermediate trifluoroacetylated nitropyrazole **8**, which was hydrolyzed in situ by rapid stirring with water to give the desired nitropyrazole **9**. Selective *N*-alkylation of **9** under Mitsunobu conditions provided exclusively regioisomer, **10**, in which alkylation occurred adjacent to the ester functionality. The use of resin bound triphenylphosphine in the Mitsunobu reaction simplified the first chromatographic purification in the reaction sequence. The purified ester **10** was hydrolyzed to acid **11** and was coupled with the aminoketone hydrochloride **12**, giving the amide **13**. The crude nitroamide **13** was then subjected to a one-pot tin(II) chloride reduction and cyclization in refluxing ethanol providing the target diazepinone **14** in about 20% overall yield from diethyl oxalate. Noteworthy is that the tin(II) chloride reduction and cyclization is absolutely critical to the successful synthesis of the diazepinone ring as reduction by Pd/C or Raney nickel provided only nitro reduction. Cyclization of the amine **13a** from these catalytic reductions was attempted without success under a variety of dehydrating conditions. Interestingly, the amine intermediate when treated with tin chloride did undergo cyclization suggesting that the aza-tin ylide **15** might be a key intermediate.

Preliminary SAR derived from the diazepinone analogs synthesized in the historic PDE4 project indicated that hydrogen bond-accepting 4-carboxyphenyl and pyridine groups were preferred aryl groups for PDE4 inhibition, while electron rich rings such as 4-methoxyphenyl favored PDE2 (Figure 4). Branched alkyl groups were preferred for PDE2 at the pyrazole 3-position, while smaller groups lead to enhanced PDE4 inhibition. 1-Ethyl pyrazole substitution was greatly preferred for PDE4 activity whereas larger or more polar groups like hydroxyethyl increased PDE2 inhibition, though the range of groups at the pyrazole N-1 position in the historic data was limited.

To begin transforming diazepinones from PDE4 selective inhibitors into a PDE2-selective series, we expanded upon the trends seen in the historical compounds. We desired to maintain drug-like attributes of **4** but also wanted to increase hydrogen bond donor count and polar surface area recognizing the need for peripherally restricted inhibitors. Thus, we targeted for synthesis compounds where the aryl group was varied and favored PDE2 inhibition in combination with either an N1 hydroxyethyl or hydroxypropyl pyrazole moiety providing compounds **16–21** (Table 1).

Clear SAR trends emerged from this first set of compounds, giving rise to diazepinones that were selective for PDE2 over PDE4. The hydroxyethyl compounds **16–18** exhibited increased inhibition of PDE2 over the hydroxypropyl analogs **19–21** (Table 1).

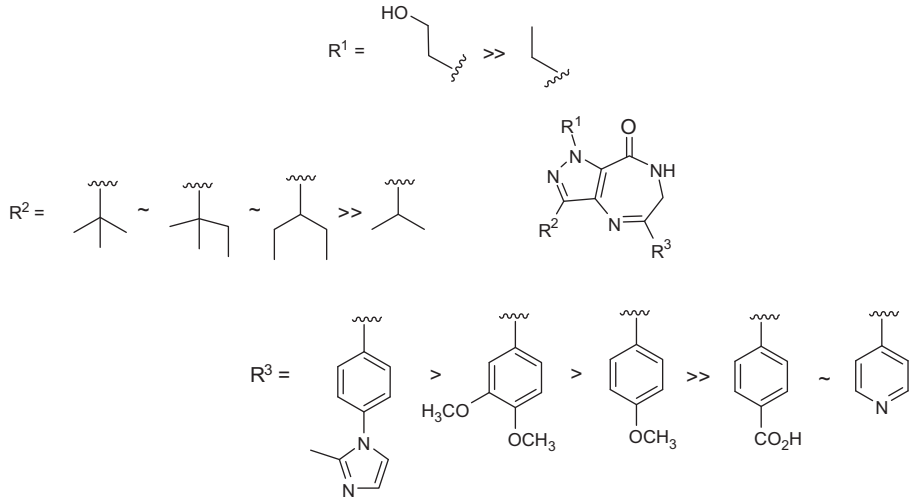

Fig. 4. PDE2 SAR from existing PDE4 inhibitors rank ordered by PDE2 inhibition.

Table 1
Diazepinone analogs targeting PDE2 activity

Ar=		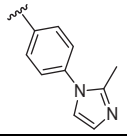	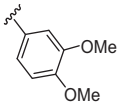	
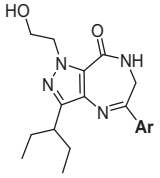	Compound	**16**	**17**	**18**
	PDE2 IC_{50} (nM)	54	23	102
	Ligand efficiency	0.32	0.36	0.38
	PDE4 IC_{50} (nM)	538	48	76
	Selectivity(PDE4/PDE2)	11	2	0.7
	HLM $t_{1/2}$ (min)	5	23	20
	*c*Log*P*	2.9	2.4	2.7
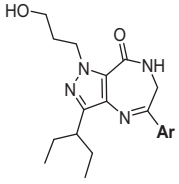	Compound	**19**	**20**	**21**
	PDE2 IC_{50} (nM)	328	93	44
	Ligand efficiency	0.28	0.32	0.33
	PDE4 IC_{50} (nM)	10800	365	1390
	Selectivity(PDE4/PDE2)	33	4	3
	HLM $t_{1/2}$ (min)	6	44	36
	*c*Log*P*	3.2	2.7	3.0

Notably the hydroxypropyl analogs were somewhat more selective. This selectivity was accomplished primarily through poorer PDE4 inhibition rather than increased PDE2 inhibition. The most selective compound **19** has modest 33-fold PDE2 selectivity and submicromolar inhibition demonstrating a good reversal of selectivity of 275-fold compared with starting PDE4 inhibitor **5**. All of the compounds, however, showed unfavorable metabolic stability, with the phenylimidazole group of **16** and **19** correlating with the poorest human liver microsome (HLM) stability. Nevertheless, the ligand efficiency of this initial set of compounds was generally greater than 0.30, the widely regarded lower limit for good lead matter.[12]

Several analogs of imidazole **16** were synthesized to determine whether sterically encumbering the imidazole group or blocking the predicted metabolically labile carbon in the 3-pentyl appendage of the pyrazole would improve metabolic stability or PDE2 selectivity (Table 2).

We attempted to improve metabolic stability by blocking the metabolically labile benzylic position in **16**, as in **22** to no avail. Neither dimethyl nor isopropyl substitution on the imidazole, as in **23** and **24**, affected metabolic stability, potency or selectivity. These observations led us to explore the more metabolically stable 3,4-dimethoxyphenyl ring in **17** and **20** even though these compounds had poor selectivity. Additionally, changing the branching of the pyrazole 3-alkyl appendage in the imidazole series offered no advantage; we opted for the tertiary butyl group as in **24** since this group has the lowest molecular weight. Although the phenylimidazole diazepinones did not provide a path forward, they demonstrated modest, reliable PDE2 selectivity and demonstrated that the PDE4 selective starting compound could be made PDE2 selective with small substituent changes. Therefore, we crystallized **22** in the PDE2 catalytic domain and determined the X-ray structure of the inhibitor-protein complex at 1.7 Å resolution, PBP ID 4JIB.

As predicted, the diazepinone PDE2 inhibitors bind to the catalytic domain in a cGMP-like binding mode shown by the orientation of Gln859 (Figure 5). The hydroxyethyl side chain points to the interior of the binding pocket, with a hydrogen bond interaction between the hydroxyl group of the inhibitor and Gln812. In PDE4, the residue corresponding to Gln812 is a proline which cannot form such a hydrogen bond. This additional interaction and the size of the surrounding pocket offer a point of differentiation, when compared to PDE4 protein and the PDE4 selective diazepinones that bind orthogonally, that contributes to the enhanced PDE2 selectivity when hydroxyl side chains are employed. The crystal structure also reveals several hydrophobic residues adjacent to the phenyl group of the phenylimidazole moiety at the entrance to the binding pocket, suggesting an additional area to further optimize PDE2 inhibition (see Part 2).

Table 2
4-Phenylimidazole SAR

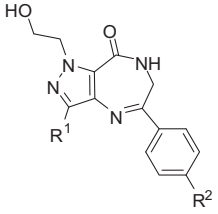

Compound	**16**	**22**	**23**	**24**
R^1		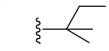		
R^2		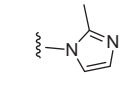	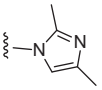	
PDE2 IC_{50} (nM)	54	45	105	97
PDE4B IC_{50} (nM)	583	378	1950	330
Selectivity	11	8	19	3
HLM $t_{1/2}$ (min)	5	7	9	12
*c*Log*P*	2.9	2.8	3.1	3.2

In summary, SAR studies of a series of pyrazolodiazepinone inhibitors selective for PDE4, having residual PDE2 activity, resulted in the discovery of a series of potent pyrazolodiazepinone inhibitors. The inhibitors possess modest selectivity and potency for PDE2 but represent a 275-fold reversal in PDE4 selectivity in favor of PDE2 selectivity. These SAR studies were based upon the hypothesis that PDE2 selectivity could be achieved with pyrazolodiazepinone inhibitors by a cGMP-like binding mode which is orthogonal to that of a cAMP binding mode seen for this family of inhibitors in PDE4. A crystal structure of a PDE2 selective inhibitor bound to the active site of the PDE2 catalytic domain is consistent with this hypothesis. Although the prototype inhibitor, **22**, possessed poor HLM stability it provided structural clues from which to build inhibitors with increased potency, selectivity and metabolic stability. Our efforts to improve the potency, selectivity, and metabolic stability of these inhibitors and to examine their

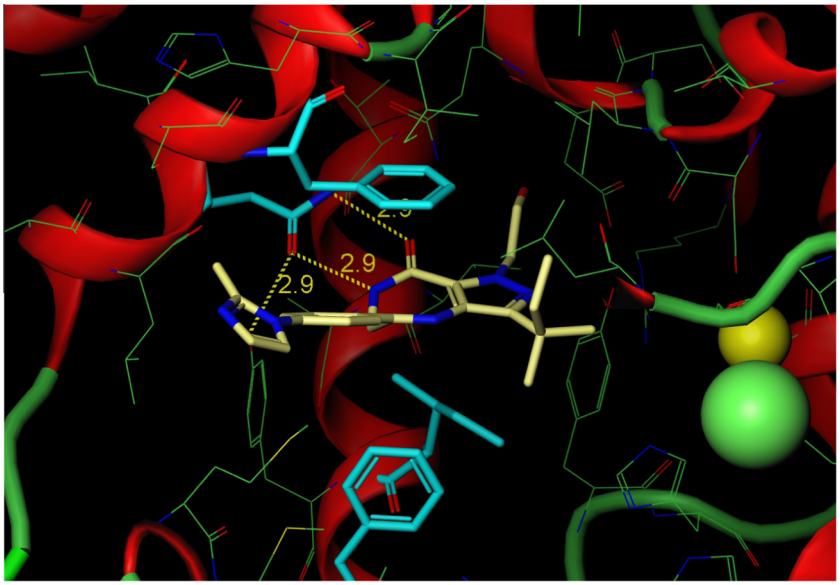

Figure 5. Crystal structure, PBP ID 4JIB, of **22** (yellow) at 1.7 Å resolution in the PDE2 catalytic domain (green) with waters removed for clarity. The conserved glutamine (Gln859), and the residues that define the 'hydrophobic clamp' (Phe862, Phe830, Ile 826) are represented as blue sticks. The two metal ions Zn (yellow) and Mg (green) are represented as spheres. Hydrogen bonding to Gln859 clearly demonstrates cGMP like orientation. An additional hydrogen bond is observed between the hydroxyethyl side chain on the inhibitor with Gln812 in the back of the binding pocket (not shown).

effects in a pain model of osteoarthritis are described in an accompanying publication.

References and notes

1. Childers, W. E.; Gilbert, A. M.; Kennedy, J. D.; Whiteside, G. T. *Expert Opin. Ther. Pat.* **2008**, *18*, 1027.
2. Chambers, R. J.; Abrams, K.; Garceau, N. Y.; Kamath, A. V.; Manley, C. M.; Lilley, S. C.; Otte, D. A.; Scott, D. O.; Sheils, A. L.; Tess, D. A.; Vellekoop, A. S.; Zhang, Y.; Lam, K. T. *Bioorg. Med. Chem. Lett.* **2006**, *16*, 307.
3. Gupta, R.; Kumar, G.; Kumar, R. S. *Methods Find Exp. Clin. Pharmacol.* **2005**, *27*, 101.
4. de Vente, J.; Markerink-van Ittersum, M.; Vles, J. S. H. *J. Chem. Neuroanat.* **2006**, *31*, 263.
5. Tegeder, I.; Schmidtko, A.; Niederberger, E.; Ruth, P.; Geisslinger, G. *Neurosci. Lett.* **2002**, *332*, 146.
6. Shi, X.; Li, X.; Clark, J. D. *Mol. Pain* **2005**, *1*, 33.
7. Podzuweit, T.; Nennstiel, P.; Muller, A. *Cell. Signalling* **1995**, *7*, 733.
8. Martinez, S. E.; Wu, A. Y.; Glavas, N. A.; Tang, X.-B.; Turley, S.; Hol, W. G.; Beavo, J. A. *PNAS* **2002**, *99*, 13260.
9. Boess, F. G.; Hendrix, M.; Van der Staay, F.-J.; Erb, C.; Schreiber, R.; van Stavern, W.; de Vente, J.; Prickaerts, J.; Blokland, A.; Koenig, G. *Neuropharmacology* **2004**, *47*, 1081.
10. Burnouf, C.; Berecibar, A.; Navet, M. *PCT Int. Appl.* **2001**, *34*, 211. WO2001049689.
11. Zhang, K. Y. J.; Card, G. L.; Suzuki, Y.; Artis, D. R.; Fong, D.; Gillette, S.; Hsieh, D.; Neiman, J.; West, B. L.; Zhang, C.; Milburn, M. V.; Kim, S.-H.; Schlessinger, J.; Bollag, G. *Mol. Cell* **2004**, *15*, 279.
12. Hopkins, A. L.; Groom, C. R.; Alex, A. Ligand efficiency: a useful metric for lead selection *Drug Disc. Today* **2004**, *9*(10), 430.

PDE2 Patent activity

(a). Bourguignon, J. -J.; Lugnier, C.; Abarghaz, M.; Lagouge, Y.; Wagner, P.; Mondadori, C.; Macher, J. -P.; Schultz, D.; Raboisson, P. WO 2004041258 A2 20040521; *PCT Int. Appl.* **2004**.

(b). Abarghaz, M.; Biondi, S.; Duranton, J.; Limanton, E.; Mondadori, C.; Wagner, P. EP 1548011 A1 20050629, *Eur. Pat. Appl.* **2005**.

(c). Schmidt, B.; Weinbrenner, S.; Flockerzi, D.; Kuelzer, R.; Tenor, H.; Kley, H. -P. WO 2006024640 A2 20060309, *PCT Int. Appl.* **2006**.

(d). Schmidt, B.; Weinbrenner, S.; Flockerzi, D.; Kuelzer, R.; Tenor, H.; Kley, H. -P. WO 2006072615 A2 20060713, *PCT Int. Appl.* **2006**.

(e). De Leon, Pablo; Egbertson, Melissa; Hills, Ivory D.; Johnson, Adam Wayne; Machacek, Michelle. WO 2011011312 A1 20110127, *PCT Int. Appl.* **2011**.

(f). Helal, Christopher John; Chappie, Thomas Allen; Humphrey, John Michael; Verhoest, Patrick Robert; Yang, Eddie. US 20120214791 A1 20120823, *U.S. Pat. Appl. Publ.* **2012**.

(g). Helal, Christopher J.; Chappie, Thomas Allen; Humphrey, John M. WO 2012168817 A1 20121213, *PCT Int. Appl.* **2012**.

(h). Niewohner, Ulrich; Schaub, Dagmar; Hendrix, Martin; Konig, Gerhard; Bos, Frank-Gerhard; Van Der Staay, Franz-Josef; Schreiber, Rudy; Schlemmer, Karl-Heinz; Grosser, Rolf. PCT WO 02/50078 A1, **2002**.

(i). Tenor, Hermann; Baer, Thomas; Hatzelmann, Armin; WO 2004/089953 A1.

(j). Niewohner, Ulrich; Bischoff, Erwin; Hutter, Joachim; Perzborn, Elisabeth; Schutz, Helmut. US 5,861,396, **1999**.

(k). Haning, Helmut; Niewohner, Ulrich; Rosentreter, Ulrich; Schenke, Thomas; Keldenich, Jorg; Bischoff, Erwin; Schlemmer, Karl-Heinz; Schutz, Helmuth; Thomas, Gunter. U.S. 6.174,884 B1, **2001**.

(l). Boss, Frank-Gerhard; Hendrix, Martin; Konig, Gerhard; Niewohner, Ulrich; Schlemmer, Karl-Heinz; Schreiber, Rudy; Van Der Staay, Franz-Josef; Schauss, Dagmar. Pub. No.: US 2002/0132754 A1, **2002**.